Available online at www.sciencedirect.com
ScienceDirect
Journal of Photochemistry and Photobiology A: Chemistry 197 (2008) 351–358
Journal of Photochemistry and Photobiology A:Chemistry
www.elsevier.com/locate/jphotochem

Covalently assembly and photophysical properties of novel lanthanide centered hybrid materials by functionalized thioacylureas bridge

Hai-Feng Lu [a], Bing Yan [a,b,*]

[a] *Department of Chemistry, Tongji University, Siping Road 1239, Shanghai 200092, China*
[b] *State Laboratory of Rare Earth Materials Chemistry and Applications, Beijing 100871, China*

Received 16 September 2007; received in revised form 11 December 2007; accepted 22 January 2008
Available online 7 February 2008

Abstract

A novel molecular precursor (abbreviated as TAM-Si) derives from thioacetaminde (TAM) modified by 3-(triethoxysilyl)-propyl isocyanate (TEPIC) though the hydrogen transfer addition reaction. Then TAM-Si behaves as functional molecular bridge which coordinates to RE^3 (Eu^{3+}, Tb^{3+}) as well as form Si—O network with inorganic precursor (TEOS) after a sol–gel process (cohydrolysis and copolycondensation reaction), resulting in the covalently bonded hybrid materials (RE–TAM-Si). On the other hand, the hybrid material of TAM-Si without introduction of RE^{3+} as well has been obtained. SEM pictures indicate that the TAM-Si show the sphere micromorphology with particle size of micrometer dimension while RE–TAM-Si hybrids present different nanometer particle, which suggests that lanthanide ions has influence on the microstructure of hybrid systems through its coordinated effect. The blue emission for TAM-Si hybrids and the narrow-width green and red emissions were achieved for Tb^{3+} and Eu^{3+} ions, respectively, indicating that the intramolecular energy transfer process take place from photoactive group to Tb^{3+} and Eu^{3+} ions in these hybrid microsphere systems. Especially the lifetime and quantum efficiency for europium hybrids have been determined.

Keywords: Molecular hybrid system; Photophysical property; Lanthanide; Thioacetaminde functionalized molecular bridge; Microsphere; Nanoparticle

1. Introduction

Recently, sol–gel derived hybrids incorporating lanthanide ions have been taken as technological potential materials in the domain of optics, especially for the fabrication of displays and lighting devices [1]. In these organic–inorganic matrices, usually designated as organically modified silicates, the thermal and mechanical stability of a siloxane-type network are combined with the multifunctional characters provided by the organic segments [2]. The desirable characteristics of polymers, namely the easy shaping, are thus brought together in a single material with the optical features provided by the luminescent centers. Lanthanide complexes have been investigated thoroughly in view of their long-lived excited-states characteristic and their especially efficient strong narrow-width emission band in the visible region [3]. Although optics might in principle be obtained in entrapping of lanthanide complexes in sol–gel derived host structures, the high decay rates of lanthanide excited states (especially deactivations associated with O—H oscillators) observed in the hybrid hosts proposed have delayed the practical application of such systems [4–7]. The disposal of linking organic and inorganic parts together with covalent bonds is a good candidate to minimize non-radiation paths, because this technology could lead to higher sample homogeneity which decreases the water molecular between organic and inorganic phases [8].

Sol–gel method has been taken as the classical approach to prepare silica-based organic–inorganic hybrid materials due to the advantages such as low-temperature processing and easy shaping, higher sample homogeneity and purity [9]. Moreover, the location of the organic segments can be priori tuned through segments-matrix interactions (covalent bonds, hydrogen bonds, ionic and van der Waals bonds) [1]. Even when all the silica materials obtained by sol–gel route are always amorphous systems, the possibility of self-organization in these hybrid materials has been demonstrated by using very specific organic precursors such as linear spacers presenting rigid or semi-rigid geometries or a di-urea based precursor that exhibit a strong interaction

* Corresponding author at: Department of Chemistry, Tongji University, Siping Road 1239, Shanghai 200092, China. Tel.: +86 21 65984663; fax: +86 21 65982287.
E-mail address: byan@tongji.edu.cn (B. Yan).

1010-6030/$ – see front matter © 2008 Elsevier B.V. All rights reserved.
doi:10.1016/j.jphotochem.2008.01.015

by H-bonding [10–12]. In all the cases investigated, only weak interactions between the organic moieties such as van der Waals, London, or π–π staking were able to induce an organization. Thus, the introduction of an organic group appeared like a factor favorable for the existence of an organization into these amorphous systems since the X-ray scattering exhibits diffraction signals, but never any Bragg peak [13].

To introduce the lanthanide complexes into the hybrids, there are many ways. One way is to utilize the coordinative site of the matrix to coordinate with lanthanide ion and combine with other ligands [14–16]. Another way is to utilize the combinable group of the complex to reaction with the siloxane hybrid precursor. The development of novel linkages for tethering organic compounds to inorganic solid supports is an area of active investigation and there are four ways to synthesis lanthanide centered luminescent hybrid materials: amino-modification [17,18], hydroxyl-modification [19–22], carboxyl-modification [23–25], and sulfonic-modification [26].

Thus, our specific investigations have concerned about the synthesis of the β-diketones siloxane hybrid precursor. The structure as well as the texture of the hybrid solids are also investigated that how the coordination between the ions and the ligands in the sol–gel process can impact on the organization in those amorphous systems. We use thioacetaminde as the original reagent. It can react with 3-(triethoxysilyl)-propyl isocyanate and the derived organosilane precursor have the functional group similar to the β-diketones [27,28]. Then the precursor was submitted to complex with Eu^{3+}/Tb^{3+} ions and to a sol–gel process in order to obtain the anticipant hybrid materials. They are generally performed at room temperature where gelatine particles have to be stabilized by chemical cross-linking. As an alternative, we developed an oil-in-water emulsion process involving the drying gelatine on a vacuum line, followed by the rapid condensation of silicates, leading to stable hybrid micro-particles. The structure of the deposited silica particles appears to depend on both organosilane concentrate and the coordination interactions.

2. Experimental

2.1. Chemicals and procedures

Starting materials were purchased from Alfa Ltd. and were used as received. All normal organic solvents were purchased from China National Medicines Group and were distilled before utilization according to the literature procedures [29]. Terbium and europium nitrates were obtained from the corresponding oxides in dilute nitric acid.

The typical procedures for the preparation of hybrid precursor and hybrid material are described in Fig. 1(I). The hybrid pre-

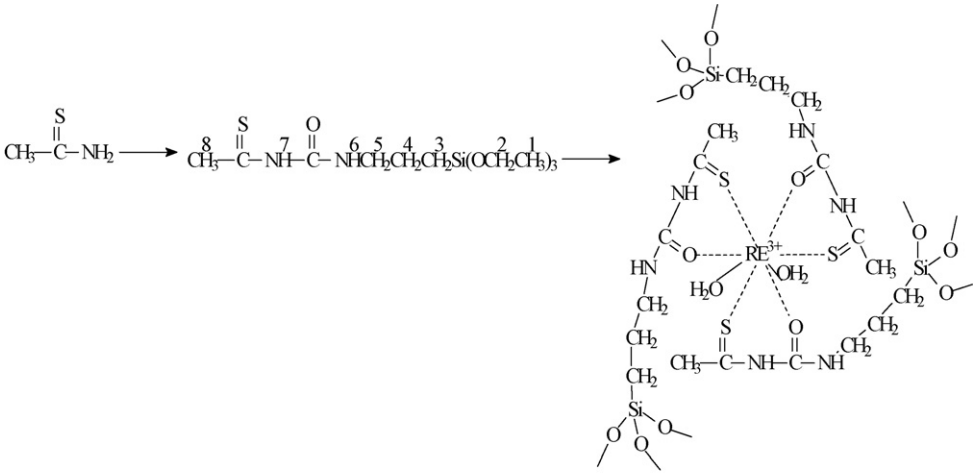

(I)

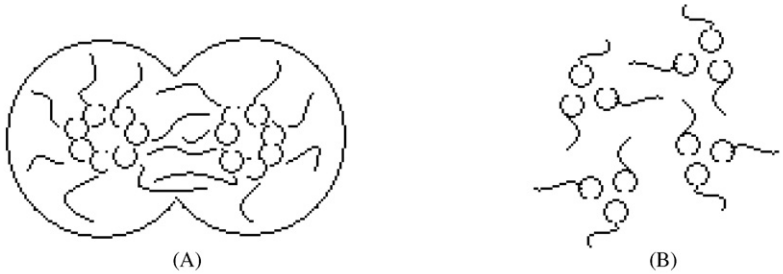

(A) (B)

(II)

Fig. 1. Scheme of (I) the typical procedures for the preparation of hybrid precursor and hybrid material and (II) the hypothetic form mechanism of TAM-Si hybrid material (A) and Eu–TAM-Si hybrid material (B).

cursor was prepared as follows: 0.45 g (6 mmol) thioacetaminde was first dissolved in 15 ml pyridine by stirring and then 1.48 g (6 mmol) 3-(triethoxysilyl)-propyl isocyanate was added to the solution by drops. The whole mixture was Refluxing at 70 °C for 6 h. The solution was condensed to evaporate the solvent and then the residue was dried on a vacuum line. A yellow oil was obtained. Anal. calcd. for $C_{17}H_{27}O_6NSSi$ (%): C 45.11, H 8.20, N 8.77; Found: C 44.85, H 7.98, N 8.54. ^{1}H NMR ($CDC1_3$, 500 MHz) 0.62 (t, 2H, H_3), 1.22 (t, 9H, H_1) 1.60 (m, 2H, H_4), 2.56 (s, 3H, H_8), 3.14 (q, 2H, H_5), 3.83 (q, 6H, H_2), 4.84 (s, 1H, H_6), 7.92 (s, 1H, H_7).

The sol–gel derived hybrid material TAM-Si was prepared as follows: 0.6 mmol hybrid precursor and 1.2 mmol tetraethoxysilane (TEOS) were dissolved in 5 ml ethanol with stirring. The mixture was agitated magnetically to achieve a single phase in a covered Teflon beaker for 4 h, and then 30 ml water was added under gentle magnetic stirring to form an initial o/w (oil-in-water) macro-emulsion for an hour. After that, it was dried on a vacuum line at 60 °C immediately. After aged until the onset of gelation which occurred, the gels were collected for the physical properties studies. It was named hybrid material I in this paper.

The sol–gel derived hybrid materials containing lanthanide ions (RE–TAM-Si, RE = Eu, Tb) were prepared as follows: 0.6 mmol sulfonamide precursor was dissolved in 5 ml ethanol with stirring. And 0.2 mmol $RE(NO_3)_3{\cdot}6H_2O$, $Tb(NO_3)_3{\cdot}6H_2O$ and $Eu(NO_3)_3{\cdot}6H_2O$, respectively) and 1.2 mmol tetraethoxysilane (TEOS) was added into the solution, respectively. The mixture was agitated magnetically to achieve a single phase in a covered Teflon beaker for 4 h, and then 30 ml water was added under gentle magnetic stirring to form an initial o/w (oil-in-water) macro-emulsion for an hour. After that, it was dried on a vacuum line at 60 °C immediately. After aged until the onset of gelation which occurred, the gels were collected for the physical properties studies.

3. Measurements

Fourier transform infrared (FTIR) spectra were measured within the 4000–400 cm^{-1} region on an (Nicolet model 5SXC) infrared spectrophotometer with the KBr pellet technique. Proton Nuclear Magnetic Resonance (^{1}H NMR) spectra were recorded in $CDCl_3$ on a BRUKER AVANCE-500 spectrometer with tetramethylsilane (TMS) as inter Reference. Elemental analyses (C, H, N) were determined with a Carlo Erba EA1110 elemental analyzer. Near Infrared spectra (NIR) of hybrid materials were recorded with a BWSpec 3.24u_58 spectrophotometer. Phosphorescent spectra (chloroform solution) and luminescence (excitation and emission) spectra of these solid complexes were determined with a RF-5301 spectrophotometer whose excitation and emission slits were 5 and 3 nm, respectively. All the emission and excitation spectra were corrected and the intensities were determined with integrated area. Luminescent lifetimes for hybrid materials were obtained with an Edinburgh Instruments FLS 920 phosphorimeter using a 450 W xenon lamp as excitation source (pulse width, 3 μs). The X-ray diffraction (XRD) measurements were carried out on powdered samples via a "BRUKER D8" diffractometer (40 mA_40 kV) using monochromated Cu Kα1 radiation (λ = 1.54 Å) over the 2θ range of 10–70°. Scanning electronic microscope (SEM) images were obtained with Philps XL-30.

4. Results and discussion

4.1. Characterization of hybrid materials

The Fourier Transform Infrared spectra (FTIR) for TAM (a), TAM-Si (b), TAM-Si hybrid material (c) and Eu–TAM-Si material (d), respectively are shown in Fig. 2. The peaks at 3200 cm^{-1} in curve of thioacetaminde is the unique vibration of NH_2 group and it turned into broad peak of ν(N–H) at 3450–3300 cm^{-1} in curve of TAM-Si (b) [25]. Two adjacent sharp peaks at 2926 and 2886 cm^{-1} in curve of TAM-Si (b) are $\nu_{as}(CH_2)$ and $\nu_s(CH_2)$ of the long carbon chain in precursors. ^{1}H NMR spectra relative to the precursors are in full agreement with the proposed structures. In the spectra of hybrid materials, the spectra are dominated by the ν(Si–O–Si) absorption bands at 1120–1000 cm^{-1}. These indicated the formation of siloxane bonds [30]. The decrease of other peaks' intensities may be due to the containing of the organic groups by the silicate inorganic host which occurred in the hydrolysis and condensation process. Coordination of lanthanide ions by the ligands is clearly shown by infrared spec-

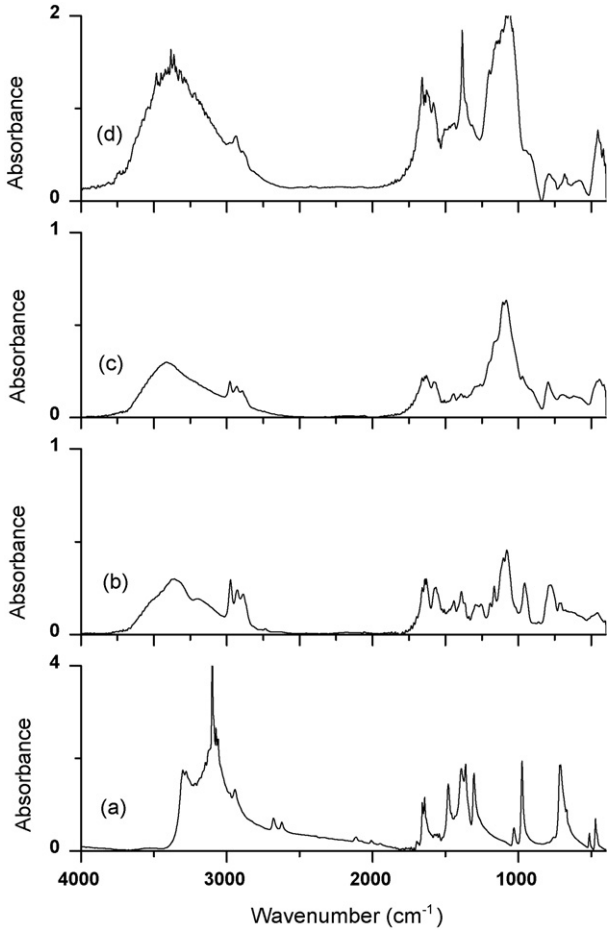

Fig. 2. Infrared spectra of thioacetaminde (a), the precursor (b), TAM-Si hybrid material (c) and Eu–TAM-Si hybrid material (d).

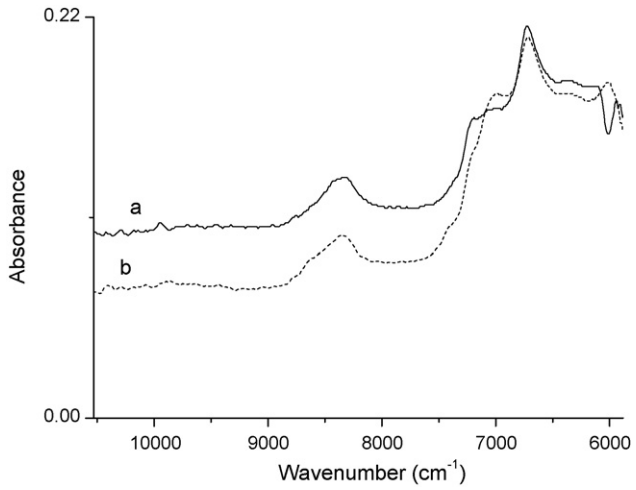

Fig. 3. Near infrared spectra of TAM-Si hybrid material (a) and Eu–TAM-Si hybrid material (b).

troscopy. In spectrum of TAM-Si (b), the ν(C=O) vibrations is located at 1686 cm^{-1}. But in the spectrum of the hybrid material II (d), the ν(C=O) vibrations is shifted to the 1596 cm^{-1} while it keep constant in the spectrum of TAM-Si (c). The shift is a proof of the coordination of the carbonyl group to the metallic ion with the oxygen atoms [20]. Fig. 3 shows the near infrared spectra (NIR) of TAM-Si (a) and Eu–TAM-Si (b). In the spectra, there is slightly difference between two curves because there is only the difference of the existence of the lanthanide ions between two kinds of hybrid materials. The shift of the broad peak from 7195–6092 to 7004–6002 nm corresponds to the coordination of lanthanide to the organic groups.

The scanning electron micrographs (SEM) of TAM-Si hybrid material (A) and Eu–TAM-Si hybrid material (B) can give some proofs from the texture (Fig. 4). For TAM-Si hybrids without lanthanide ions, in the sol process, the o/w macro-emulsion is decisive and responsibility for the hybrids' final texture. The isolated sphere is easy to understand because the weak interactions between the organic moieties such as van der Waals, London, or π–π staking were able to induce an organization [10–12]. For the bi-sphere particle, it may be supposed that pervasions take place between two spheres (see A in Fig. 1(II)). The microsphere is located in 2–5 μm dimension. The micromorphology of Eu–TAM-Si introduced europium ions seems to be largely different with TAM-Si while they were prepared by same process, whose particle sizes are in the 50–100 nm dimension. Because of the strong chelation effect between organic groups and lanthanide ions, the configurations of the organosilane is mixed up and it is difficult to form an organization under the weak interactions such as π–π staking (as shown the hypothesis in Fig. 1(II, B)).

As mentioned in the experimental, the hybrid materials could be received through a polycondensation reaction between the terminal silanol groups of TAM-Si and the OH groups of hydrolyzed TEOS. The possible reaction model of TEOS and TAM-Si were illustrated in Fig. 4. At the beginning of the reaction, as shown in Fig. 4 (Step I), the individual hydrolysis of TAM-Si and TEOS are predominant. The Steps II and III,

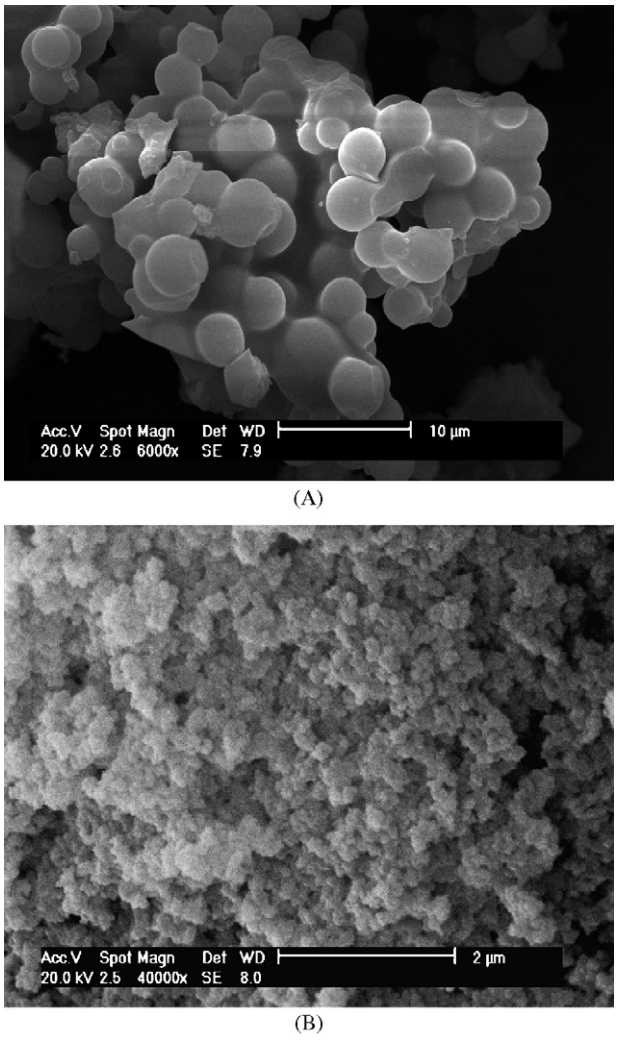

Fig. 4. The scanning electron micrographs of (A) TAM-Si hybrid material and (B) Eu–TAM-Si hybrid material.

however, are related to the polycondensation reactions between hydroxyl groups of both TMASi and TEOS. By these methods, the covalently bonded hybrids TAM-Si can be achieved. Similarly, the molecular-based composites bearing the RE–O coordination bond and Si–O covalent bonds can also been obtained after the introduction of RE^{3+}. Here we named the cooperation of both TMASi and TEOS within the in situ sol–gel process as cohydrolysis and copolycondensation (similar to copolymerization of organic monomer). Compared the TMA-Si without RE^{3+} and RE–TMA-Si hybrids, there exists the apparent distinction. The former only involves the sol–gel process (cohydrolysis and copolycondensation process), while the latter appears coordination reaction between RE^{3+} and TMASi, which have great influence on the sol–gel process and the microstructure or physical properties of the hybrids. For TMS-Si hybrids, the generously sol–gel process is favorable for the mass transport and particle growth, resulting in the larger particle size of microstructure. Besides, the uniformly growth without any other interaction becomes easy for sol–gel process, so the large particle of sphere microphology can form. Because the sol–gel process involves two precursors, TMASi and TEOS, so it is

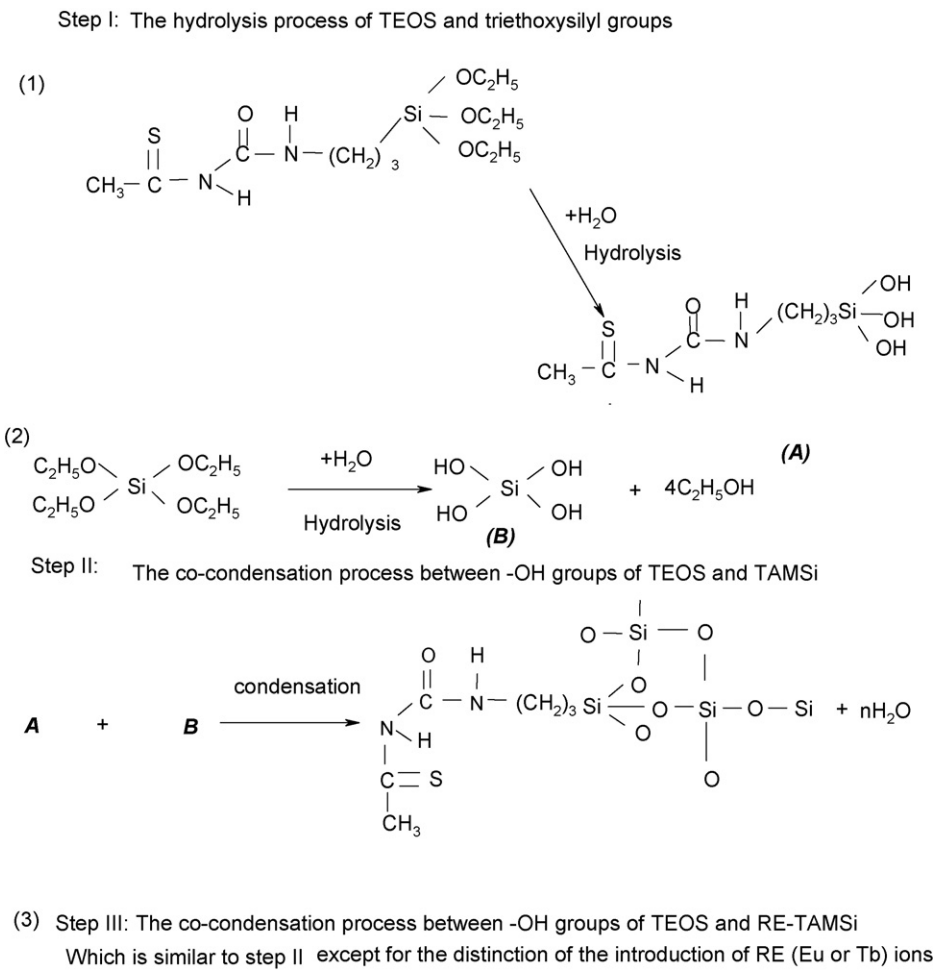

Fig. 5. The scheme of hydrolysis and polycondensation processes between TAM-Si (or RE–TAM-Si) and TEOS.

easy to understand that the cohydrolysis and copolycondensation process from different precursor each other give rise to the biosphere microstructure. For RE–TMA-Si hybrids, when RE^{3+} (Eu^{3+} or Tb^{3+}) was introduced, the chelation effect between RE^{3+} and TMASi naturally influences on the hydrolysis and polycondensation process of TMASi directly, further influence on the growth tendency or rate of the final hybrids, which can control the microstructure and luminescent properties of them. As we know, RE^{3+} possesses the high coordination number, so the chelated ability is strong and can play a role in the control of hybrids. Subsequently, the coordination effects intervene the normal sol–gel process and limits growth rate and particle size. The interpretation has been verified from the above SEM patterns and the below luminescent properties (Fig. 5).

4.2. Photophysical properties of hybrid materials

Carbonyl and thiocarbonyl compounds are already well known to be good chelating groups to sensitize luminescence of lanthanide ions. The mechanism usually described as antenna effect: the ligand reinforce the energy absorbability and transfer it to the metal ion with high efficiency. Then the emission from the lanthanide ions' excited state will be observed [31]. The phosphorescence spectra of TAM (a) and the precursor TAM-Si (b) are recorded in Fig. 6. All of the curves exhibited a broad phosphorescence band which corresponds to the triplet state emission of them. A red shift was observed between thioacetaminde TAM and precursor because the modification

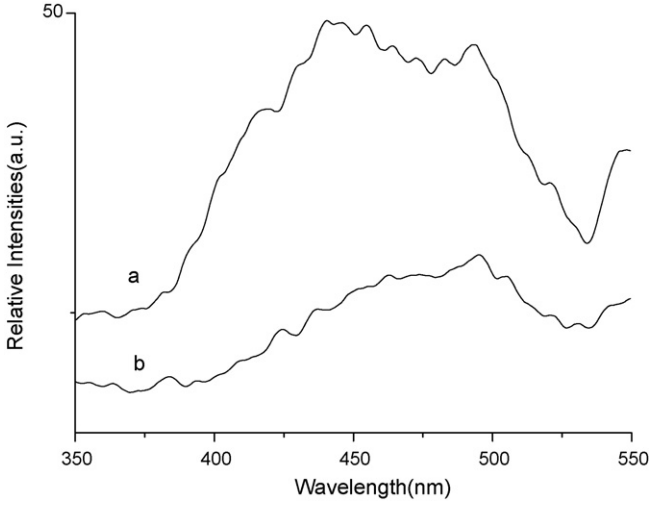

Fig. 6. Phosphorescence spectra of thioacetaminde TAM (a) and the precursor TAM-Si (b).

of thioacetaminde enlarges the conjugation. The triplet state energy of carbonyl group is 22,720 cm^{-1} for TAM-Si and energy differences between it and the resonant emissive energy levels of terbium ion (20,500 cm^{-1}) or (europium ion (17,300 cm^{-1})) are 2220 and 5420 cm^{-1}, respectively. According to the energy transfer and intramolecular energy mechanism [32–35], the intramolecular energy transfer efficiency depends on energy difference, whose value is neither more nor less. So it can be predicted that the triplet state energy of precursor is quite suitable for the luminescence of terbium ion but poor for europium ion for the energy difference for Eu^{3+} is too larger. When the gap of the energy levels between the ligand and europium ion is large, the energy transfer will be hampered.

Fig. 7 is the excitation spectra of the resulting hybrid materials, which are monitored at 545 nm under room temperature. The spectra exhibits broad excitation bands centered at 330 nm in the UV range, respectively. The band around 330 nm corresponds to ligand-to-metal charge transfer (LMCT) transition caused by interaction between the organic groups and the lanthanide ions [35]. No f–f transitions could be observed in the spectra. The luminescence behaviors of all of the materials have been investigated at 298 K by direct excitation of the ligands (330 nm). Representative emission spectra are given in Figs. 8–10, respectively. It is a narrow-width red emission of europium hybrid materials. The narrow-width green emission is observed in the terbium hybrid materials. Fig. 9 illustrates typical photoluminescence spectra of the hybrid material I. Because no lanthanide ions are doped in them, this kind of hybrid materials can only emit the luminescence of the organic group. The peak of the emission is located at 467 nm. Fig. 9 illustrates typical photoluminescence spectra of the europium hybrid material. The maxima of these bands are at 590 and 613 nm which is associated with $^5D_0 \rightarrow {}^7F_1$ and $^5D_0 \rightarrow {}^7F_2$ transitions, respectively. The energy transfer from the carboxylic ligand to europium(III) is not perfect, as can be noticed to the residual ligand emission between 500 and 570 nm. It is not surprise because the poor energy level match has been described previously. A prominent feature that may be noted in these spec-

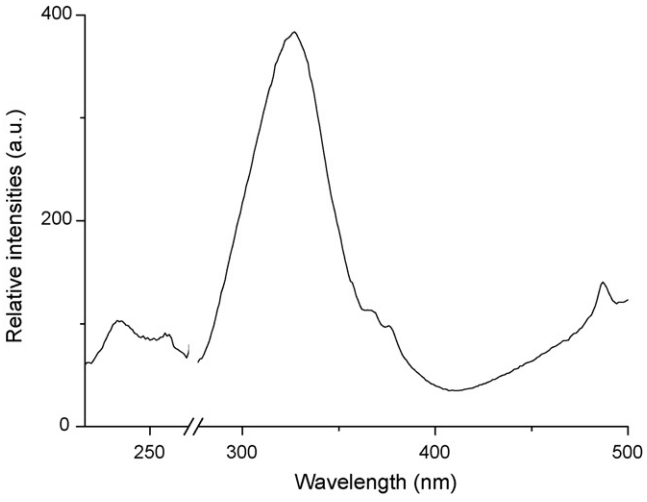

Fig. 7. The excitation spectra of TAM-Si hybrid material.

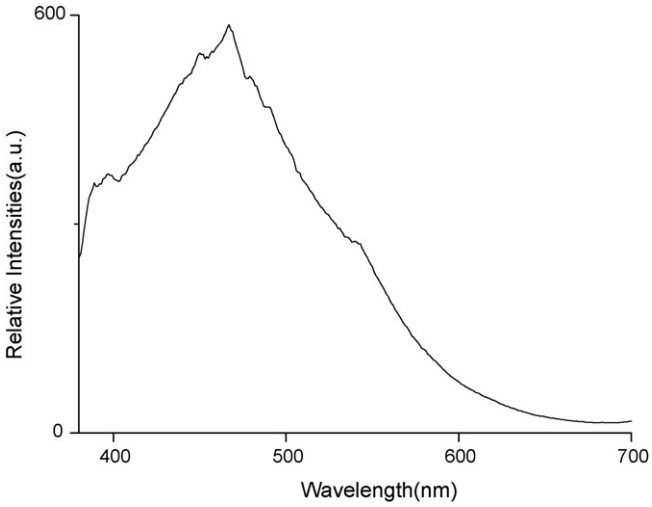

Fig. 8. The emission spectra of TAM-Si hybrid material.

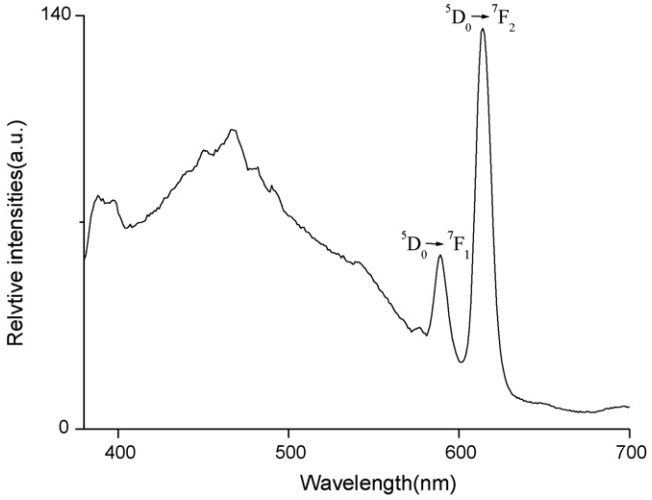

Fig. 9. The emission spectra of Eu–TAM-Si hybrid material.

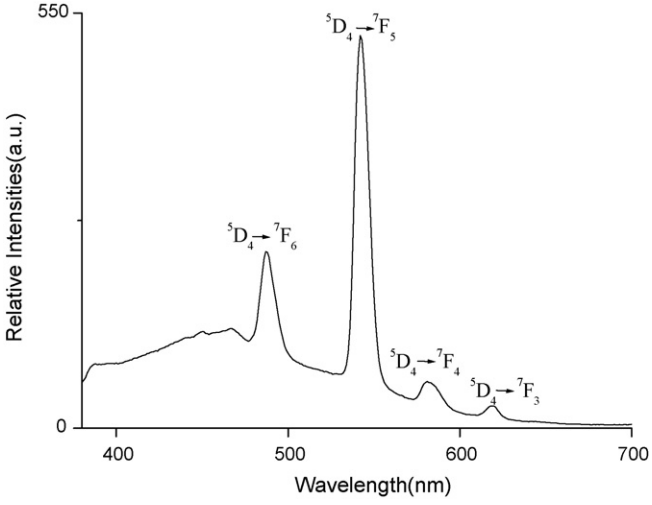

Fig. 10. The emission spectra of Tb–TAM-Si hybrid material.

Table 1
Luminescent data for the covalently bonded europium and terbium hybrid materials.

Molecular hybrids	Eu–TAM-Si	Tb–TAM-Si
Emission band (nm)	577, 589, 614, 647, 696 17331, 16978, 16287, 15456, 14368	487, 542, 581, 619
Relative intensities (a.u.)[a]	3.45, 28.95, 125.69, 0.90, 0.78	233, 520, 52.6, 24.5
Lifetimes (ms)[b]	0.44	0.81
Experimental decay rates (s^{-1})	2273	
Radiative decay rates (s^{-1})	285.43	
Non-radiative decay rates (s^{-1})	1987.57	
Number of coordinated water	2.09	
Quantum efficiency (%)	12.56	

[a] The relative intensities were obtained by the calculation of integral area of the same emission bands.
[b] For $^5D_0 \rightarrow {}^7F_2$ transition of Eu^{3+}.

tra is the high intensity ratios of $I(^5D_0 \rightarrow {}^7F_2)/I(^5D_0 \rightarrow {}^7F_1)$. The intensity (the integration of the luminescent band) ratio of the $^5D_0 \rightarrow {}^7F_2$ transition to $^5D_0 \rightarrow {}^7F_1$ transition has been widely used as an indicator of Eu^{3+} site symmetry [36]. When the interactions of the lanthanide complex with its local chemical environment are stronger, the complex becomes more nonsymmetrical and the intensity of the electric–dipolar transitions becomes more intense. As a result, $^5D_0 \rightarrow {}^7F_1$ transition (magnetic–dipolar transitions) decreased and $^5D_0 \rightarrow {}^7F_2$ transition (electric–dipolar transitions) increased. In this situation, the intensity ratios are approximately 2.5. This ratio is only possible when the europium ion does not occupy a site with inversion symmetry [35]. It is clear that the strong coordination interactions took place between the organic groups and lanthanide ions. Fig. 10 illustrates typical photoluminescence spectra of the terbium hybrid material. Narrow-width emission bands with maxima at 487, 543, 580 and 619 nm are recorded. These bands are related to the transition from the triplet state energy level of Tb^{3+} to the different single state levels and are attributed to the $^5D_4 \rightarrow {}^7F_6$, $^5D_4 \rightarrow {}^7F_5$, $^5D_4 \rightarrow {}^7F_4$ and $^5D_4 \rightarrow {}^7F_3$ transitions of Tb^{3+} ions. The lower baseline in the spectra suggests that energy transfer efficiency between the organic groups and Tb^{3+} ions is higher than that between the organic groups and Eu^{3+} ions. Base on the above results, three covalently bonded hybrid materials can be achieved through the one modified functional derivatives and sol–gel technology, which exhibit three different kinds of luminescence (trichromatic luminescence of blue, green and red). It can be predicted to modify the molar ratio of three hybrids and assembled them in one hybrid Si–O hybrid network systems through the cohydrolysis and copolycondensation process, resulting in the white luminescence. This however needs to be fundamentally investigated further.

The typical decay curve of the Eu and Tb hybrid material were measured and they can be described as a single exponential ($\mathrm{Ln}(S(t)/S_0) = -k_1 t = -t/\tau$), indicating that all Eu^{3+} and Tb^{3+} ions occupy the same average coordination environment. The resulting lifetimes of Eu and Tb hybrids are given in Table 1. We further determined the emission quantum efficiencies of the $^5D_0$ europium ion excited state for Eu^{3+} hybrids on the basis of the emission spectra and lifetimes of the $^5D_0$ emitting level using the four main equation according to the Ref. [37–45]. The detailed principle and method was adopted as Ref. [42] and the data are shown in Table 1.

$$A_{0J} = A_{01}\left(\frac{I_{0J}}{I_{01}}\right)\left(\frac{\upsilon_{01}}{\upsilon_{0J}}\right) \quad (1)$$

$$A_{\mathrm{rad}} = \sum A_{0J} = A_{00} + A_{01} + A_{02} + A_{03} + A_{04} \quad (2)$$

$$\tau = A_{\mathrm{rad}}^{-1} + A_{\mathrm{nrad}}^{-1} \quad (3)$$

$$\eta = \frac{A_{\mathrm{rad}}}{A_{\mathrm{rad}} + A_{\mathrm{nrad}}} \quad (4)$$

Here A_{0J} is the experimental coefficients of spontaneous emissions, among A_{01} is the Einstein's coefficient of spontaneous emission between the $^5D_0$ and $^7F_1$ energy levels, which can be determined to be $50\,s^{-1}$ approximately [42–45] and as a reference to calculate the value of other A_{0J}. I is the emission intensity and can be taken as the integrated intensity of the $^5D_0 \rightarrow {}^7F_J$ emission bands [38,39]. υ_{0J} Refers to the energy barrier and can be determined from the emission bands of Eu^{3+}'s $^5D_0 \rightarrow {}^7F_J$ emission transitions. A_{rad} and A_{nrad} mean to the radiative transition rate and nonradiative transition rate, respectively, among A_{rad} can be determined from the summation of A_{0J} (Eq. (2)). And then the luminescence quantum efficiency can be calculated from the luminescent lifetimes, radiative and nonradiative transition rates. The luminescent quantum efficiency for europium hybrid Eu–TAM-Si is estimated as 12.56, which directly be due to the short luminescent lifetimes. The low quantum efficiency for Eu–TAM-Si indicates that the energy match and energy transfer between TAM-Si and Eu^{3+} is not effective, which take agreement with the prediction of above discussion. Although the quantum efficiency of Tb system is too complicated to be calculated from the lifetime data of Tb–TAM-Si hybrids, we still predict that the quantum efficiency for terbium hybrids may be higher than europium one because it possess longer lifetime (0.81 ms).

Horrocks and Sudnick suggested that the number of water molecules coordinated to the metal ion (n_{w}) could be evaluated according to the empirical formula [46].

$$n_{\mathrm{w}} = 1.05A_{\mathrm{nrad}} = 1.05(A_{\mathrm{exp}} - A_{\mathrm{rad}}) = 1.05(\tau_{\mathrm{exp}}^{-1} - A_{\mathrm{rad}}) \quad (5)$$

It is found that the number of water molecules belonging to the Eu^{3+} first coordination shell is similar for both the complex and

the nanocomposite [41]. Therefore, we can determine that the number of coordinated water molecules to Eu^{3+} is 2 (as shown in Fig. 1(I)). The two water coordinated water molecules maybe the main factor to decrease the energy transfer efficiency and luminescent quantum efficiency.

5. Conclusions

In this work, three novel kinds covalently boned hybrid materials with blue (TAM-Si), green (Tb–TAM-Si) and red (Eu–TAM-Si) luminescence have been prepared by sol–gel process based on an o/w process and organosilane polycondensation. The coordination between the ions and the ligands in the sol–gel process can impact on the organization in those amorphous systems as well on the luminescent behaviors.

Acknowledgement

This work was supported by the National Natural Science Foundation of China (20671072).

References

[1] C. Sanchez, B. Lebeau, F. Chaput, J.P. Boilot, Adv. Mater. 15 (2003) 1969–1994.
[2] M.C. Goncalves, N.J.O. Silva, V.D.Z. Bermudez, R.A.S. Ferreira, L.D. Carlos, K. Dahmouche, C.V. Santilli, D. Ostrovskii, I.C.C. Vilela, A.F. Craievich, J. Phys. Chem. B 109 (2005) 20093–20104.
[3] L.R. Matthews, E.T. Knobbe, Chem. Mater. 5 (1993) 1697–1703.
[4] C. Sanchez, F. Ribot, R. Lebeau, J. Mater. Chem. 9 (1999) 35–44.
[5] L.D. Carlos, R.A.S. FerReira, V.D. Bermudez, Electrochim. Acta 45 (2000) 1555–1560.
[6] K. Driesen, R.V. Deun, C. Gorller-Walrand, K. Binnemans, Chem. Mater. 16 (2004) 1531–1535.
[7] L.N. Sun, H.J. Zhang, Q.G. Meng, F.Y. Liu, L.S. Fu, J.B. Yu, C.Y. Peng, G.L. Zheng, S.B. Wang, J. Phys. Chem. B 109 (2005) 6174–6182.
[8] Q.M. Wang, B. Yan, Inorg. Chem. Commun. 7 (2004) 1124–1127.
[9] U. Schubert, N. Husing, A. Lorenz, Chem. Mater. 7 (1995) 2010–2027.
[10] A. Shimojima, Y. Sugahara, T. Ohsuna, O. Terasakl, Nature 416 (2002) 304–306.
[11] J.J.E. Moreau, L. Vellutim, M.W.C. Man, C. Bied, J. Am. Chem. Soc. 123 (2001) 1509–1510.
[12] J.J.E. Moreau, L. Vellutim, M.W.C. Man, C. Bied, J.L. Bantignles, P. Dieudonne, J.L. Sauvajol, J. Am. Chem. Soc. 123 (2001) 7957–7958.
[13] G. Cerveau, R.J.P. Corriu, E. Framery, F. Lerouge, Chem. Mater. 16 (2004) 3794–3799.
[14] H.R. Li, J. Lin, H.J. Zhang, L.S. Fu, Q.G. Meng, S.B. Wang, Chem. Mater. 14 (2002) 3651–3655.
[15] K. Binnemans, P. Lenaerts, K. Driesen, C. Gorller-Walrand, J. Mater. Chem. 14 (2004) 191–195.
[16] P. Lenaerts, A. Storms, J. Mullens, J. Dhaen, C. Gorller-Walrand, K. Binnemans, K. Driesen, Chem. Mater. 17 (2005) 5194–5201.
[17] Q.M. Wang, B. Yan, J. Mater. Chem. 14 (2004) 2450–2455.
[18] F.F. Wang, B. Yan, J. Organomet. Chem. 692 (2007) 2395–2402.
[19] Q.M. Wang, B. Yan, J. Organomet. Chem. 691 (2006) 540–545.
[20] Q.M. Wang, B. Yan, J. Organomet. Chem. 691 (2006) 3567–3573.
[21] D.J. Ma, B. Yan, J. Solid State Chem. 179 (2006) 2059–2066.
[22] X.F. Qiao, B. Yan, Photochem. Photobiol. 83 (2007) 971–978.
[23] Q.M. Wang, B. Yan, Cryst. Growth Des. 5 (2006) 497–503.
[24] Q.M. Wang, B. Yan, J. Mater. Res. 20 (2006) 592–598.
[25] Q.M. Wang, B. Yan, J. Photochem. Photobiol. A Chem. 175 (2006) 159–165.
[26] H.F. Lu, B. Yan, J. Non-Cryst. Solids 352 (2006) 5331–5335.
[27] B. Klaus, H. Eva, Chemiker-Zeitung 112 (1988) 349–357.
[28] V.I. Cohen, J. Org. Chem. 39 (1974) 3043–3048.
[29] D.D. Perrin, W.L.F. ArmaRego, D.R. Perrin (Eds.), Purification of Laboratory Chemicals, Pergamon Press, Oxford, 1980.
[30] E. Pretsch, P. Buhlmann, C. Affolter (Eds.), Structure Determination of Organic Compounds, Springer, Berlin, 2003 (2nd printing).
[31] J. Genzer, J. Groenewold, Soft Matter 2 (2006) 310–319.
[32] S. Sato, M. Wada, Bull. Chem. Soc. Jpn. 43 (1970) 1955–1964.
[33] Q.M. Wang, B. Yan, X.H. Zhang, J. Photochem. Photobiol. A Chem. 174 (2005) 119–124.
[34] B. Yan, B. Zhou, J. Photochem. Photobiol. A Chem. 171 (2005) 181–186.
[35] S.L. Wu, Y.L. Wu, Y.S. Yang, J. Alloys Compds. 180 (1994) 399–403.
[36] Z. Wang, J. Wang, H.J. Zhang, Mater. Chem. Phys. 87 (2004) 44–48.
[37] O.L. Malta, M.A.C. dos Santos, L.C. Thompson, N.K. Ito, J. Lumin. 69 (1996) 77–84.
[38] O.L. Malta, H.F. Brito, J.F.S. Menezes, F.R.S. Goncalvese, A.F.S. Farias, A.V.M. Andrade, J. Lumin. 75 (1997) 255–268.
[39] L.D. Carlos, Y. Messaddeq, H.F. Brito, R.A. Sa Ferreira, V.D.Z. Bermudez, S.J.L. Ribeiro, Adv. Mater. 12 (2000) 594–598.
[40] R.A.S. Ferreira, L.D. Carlos, R.R. Goncalves, S.J.L. Ribeiro, V.D. Bermudez, Chem. Mater. 13 (2001) 2991–2998.
[41] P.C.R. Soares-Santos, H.I.S. Nogueira, V. Felix, M.G.B. Drew, R.A.S. Ferreira, L.D. Carlos, T. Trindade, Chem. Mater. 15 (2003) 100–108.
[42] E.E.S. Teotonio, J.G.P. Espynola, H.F. Brito, O.L. Malta, S.F. Oliveria, D.L.A. de Faria, C.M.S. Izumi, Polyhedron 21 (2002) 1837–1844.
[43] S.J.L. Ribeiro, K. Dahmouche, C.A. Ribeiro, C.V. Santilli, S.H.J. Pulcinelli, J. Sol–Gel Sci. Technol. 13 (1998) 427–432.
[44] M.H.V. Werts, R.T.F. Jukes, J.W. Verhoeven, Phys. Chem. Chem. Phys. 4 (2002) 1542–1548.
[45] C.Y. Peng, H.J. Zhang, J.B. Yu, Q.G. Meng, L.S. Fu, H.R. Li, L.N. Sun, X.M. Guo, J. Phys. Chem. B 109 (2005) 15278–15287.
[46] W.D. Horrocks Jr., W.D.R. Sudnick, Acc. Chem. Res. 12 (1981) 384–392.